Meat Science 234 (2026) 110048

Contents lists available at ScienceDirect

Meat Science

journal homepage: www.elsevier.com/locate/meatsci

Non-invasive detection of cold chain disruptions in modified-atmosphere packaged minced pork using a handheld fluorescence device

Johannes Schlosser [a], Martin Mühling [b], Sonja Lick [b], Heinar Schmidt [a,*]

[a] Chair of Bioanalytical Sciences and Food Analysis, University of Bayreuth, Fritz-Hornschuch-Str. 9, 95326 Kulmbach, Germany
[b] Max Rubner-Institute, Federal Research Institute of Nutrition and Food, Department of Safety fand Quality of Meat, E.-C.-Baumann-Str. 20, 95326 Kulmbach, Germany

ARTICLE INFO

Keywords:
Cold chain interruption
Spectroscopic detection
Storage time
Total viable count
MAP meat

ABSTRACT

This study demonstrates the suitability of a handheld fluorescence device for the detection of cold chain disruptions (CCDs) of modified-atmosphere packaged minced pork through the package or with unpacked samples. Fluorescence spectra of minced pork stored at a constant temperature of 2 °C were highly correlated with the storage time after processing of the meat. Partial least squares regression (PLSR) models for spectra recorded through the package or for unpacked samples yielded cross-validated $R^2_{CV} = 0.90$ or 0.95, respectively. Validation with independent samples investigated under controlled conditions resulted in $R^2_{Pred} = 0.83$ for measurements through the package and 0.88 for measurements of unpacked samples. Unlike the controls, minced pork, which underwent a CCD at 14 °C on storage day 2, was systematically predicted older than its actual storage time depending on the duration of the disruption: 1.1–1.7 d older after a 6-h disruption and with 2.5–3.5 d significantly older after a 12-h disruption. In contrast, CCD-dependent changes of total viable counts (TVC) only appeared on tendency after a 12-h CCD and PLSR predictions of TVC performed inadequately. The storage-time effect detected by fluorescence spectroscopy was apparent already one day after the disruption. The results indicate that fluorescence spectra monitor an ageing process of meat, which is accelerated by a temporarily elevated storage temperature. The comparison of predicted and actual storage time could be useful for a rapid, non-invasive detection of cold chain disruptions and for an assessment of time and temperature effects on the shelf life.

1. Introduction

Perishable food such as fresh meat or minced meat requires cold storage to maintain freshness and shelf life of the products. Therefore, an uninterrupted cold chain is an important component to protect the health of consumers (Bartáková et al., 2022; Bruckner, Albrecht, Petersen, & Kreyenschmidt, 2012; Deng et al., 2024; EFSA Panel on Biological Hazards, 2016; Necidová et al., 2024). European law stipulates that foodstuffs susceptible to the reproduction of pathogenic microorganisms or the formation of toxins must not be subjected to any unjustified interruption of the cold chain (Regulation (EC) No 852/2004, 2004a). Hence, it is common practice to monitor storage temperatures with temperature loggers, which are installed in the cold stores and transport vehicles (D. Kumar, Singh, & Layek, 2020). However, this has weak points. Due to temperature fluctuations inside the cold store, for example a lorry, the measured temperatures do not necessarily correspond to the actual temperature of the stored product (So, Joe, Hwang, Jun, & Lee, 2021). Technical faults or deliberate deception can lead to incomplete or manipulated data. To overcome these limitations, methods are required, which are operating on the level of the product and independent of a temperature logger. Previous research has primarily focused on the application of intelligent packaging where a disruption is detected by the package or a device attached to the package (Albrecht et al., 2020; Pandian, Chaturvedi, & Chakraborty, 2021; Yousefi et al., 2019). Disadvantages of these methods are among other the additional costs of the packaging (Sohail, Sun, & Zhu, 2018). Wang et al. demonstrated direct detection of cold chain disruptions in lean and fatty pork by extracting specific spoilage markers from metabolites and analyzing them through subsequent MS/MS analysis (Wang, Jiang, Zhang, Zhu, & Wu, 2025). However, this procedure is time-consuming, destructive and involves a high investment in equipment. As an alternative, spectroscopic approaches allow non-destructive measurements through a package. Turgut et al. investigated cold chain disruptions including a thawing and refreezing processes by a portable

* Corresponding author.
E-mail address: heinar.schmidt@uni-bayreuth.de (H. Schmidt).

https://doi.org/10.1016/j.meatsci.2026.110048
Received 7 August 2025; Received in revised form 24 January 2026; Accepted 26 January 2026
Available online 31 January 2026

spectrometric system (Turgut, Myustedzhebov, & Feyissa, 2025). They detected changes in the VIS-NIR reflectance of thawed and then frozen meat and explained them by the formation of larger ice crystals during refreezing and an accelerated lipid, protein and myoglobin oxidation as well as protein denaturation (Turgut et al., 2025). However, this approach is not applicable to products which are not frozen, such as fresh or minced meat. To the best of our knowledge, no studies have yet investigated whether fluorescence spectroscopy can detect temporary interruptions to the cold chain during the storage of meat.

In the past decades, various spectroscopic methods have been scrutinized to assess meat quality and spoilage, including VIS-NIR HSI (Jo et al., 2024), FTIR (Candoğan, Altuntas, & İğci, 2021) and Raman spectroscopy (Qu et al., 2022). Among these rapid methods, fluorescence spectroscopy was identified as suitable for the assessment of ageing and quality parameters of fresh meat using protoporphyrin IX (PPIX) and Zn protoporphyrin IX (Zn-PPIX) as indicators (Schneider et al., 2008). Subsequent work with pork stored under different packaging and storage conditions showed that the fluorescence of Zn-PPIX at 590 nm was related to increasing spoilage of the meat and the authors concluded that fluorescence spectroscopy has potential to indicate remaining shelf life (Durek, Bolling, Knorr, Schwägele, & Schlüter, 2012). However, fluorescence intensities were modulated by the type of packaging: intensities were largest when the meat was stored in vacuum, intermediate when aerobically stored, but strongly reduced in high oxygen modified-atmosphere packaging (MAP) due to quenching by oxygen (Durek et al., 2012). Oto et al. predicted ATP content and total aerobic plate count (TVC) for pork stored aerobically at 15 °C within the first 72 h using fluorescence spectroscopy (Oto et al., 2013). Subsequent work showed that porphyrin fluorescence could also be detected in pork and lamb with a hand-held device that used a diode laser emitting at 405 nm as light source. This device was specifically developed for monitoring of microbial contamination (Durek et al., 2016). Grimmler et al. demonstrated the prediction of TVC of minced pork stored aerobically at 2 °C for 8 days using a commercial hand-held fluorescence device with 405 nm excitation (Grimmler, Kuhfuß, Heiden, & Schmidt, 2018). The authors found similar cross-validated partial least squares (PLS) correlations of the fluorescence spectra with TVC and with storage time ($R^2_{cv} = 0.81$ and $R^2_{cv} = 0.86$, respectively), and they reported correlations between TVC and storage time (r^2 in the range 0.55–0.77) (Grimmler et al., 2018). Such storage tests are conducted at a constant (low) temperature by design and, therefore, log-transformed TVC are linearly dependent on the storage time during the exponential growth phase of the microbiota. The question of the extent to which the fluorescence of the porphyrins is related to TVC or to the storage time could not be answered. Publications targeting different storage temperatures are rare in this field. Fengou et al. reported experiments with aerobically and modified-atmosphere packaged (MAP) minced pork patties stored isothermically at 4, 8 and 12 °C and under a dynamic temperature condition, which was alternating the three temperatures every 8 h. They used Fourier transform infrared spectroscopy (FTIR) and multispectral imaging (MSI) in combination with machine learning to estimate the total mesophilic microbial load, and reported root mean squared errors (RMSE) of the correlations between 0.9 and 2.3 log(cfu/g) depending on packaging type and dimensionality-reduction method (Fengou, Mporas, Spyrelli, Lianou, & Nychas, 2020). This work showed the feasibility to estimate TVC from spectral data for storage at different temperatures, but the RMSEs were unsatisfactorily high.

This study aimed at investigating how fluorescence spectra are affected by non-constant storage temperatures. Specifically, we used modified-atmosphere packaged minced pork as a food model to assess whether cold chain disruption could be detected by fluorescence spectroscopy and whether this could be achieved non-invasively through the package, or only once the sample had been unpacked. Given the relationship between storage time and microbial growth, we also monitored and correlated the total viable (aerobic) plate count (TVC) with fluorescence spectra. Thus, this study should also help to answer the question as to what extent porphyrin fluorescence in meat products is related to TVC and storage time.

2. Experimental

This feasibility study was designed to determine whether fluorescence spectroscopy could genuinely detect the impact of a CCD and thus help to reduce food waste. The point in time for the CCD was selected based on a scenario of a failure of the cooling system such as of a transport lorry early in the supply chain, that is within the first 4 days. During this period, the packages are usually transported twice in an industrial production process: first to a central warehouse and then to the retailer. The middle of this period was chosen. At that stage, the microbiota associated with the meat product are generally still in the lag phase of growth. The effect of the CCD is expected to be less pronounced than if it occurred at the start of, or during the exponential growth phase. The temperature to which the minced pork samples were exposed during the CCD was intentionally chosen lower than expected in a worst-case scenario (e.g. cooling system failure on hot summer days). The cooling failure duration of 6 h was estimated as time frame required to transfer the cargo to another refrigerated place, and 12 h was selected to achieve a significant time-temperature effect in the product. The average duration of refrigerated transport typically ranged from 6 to 8 h (Derens-Bertheau, Osswald, Laguerre, & Alvarez, 2015). It is noted that studies on the time-temperature management of the cold chain identified rather shorter periods of temperature abuses mostly during loading and unloading of the transport vehicles, in the display cabinets during retail and during domestic refrigeration (Mercier, Villeneuve, Mondor, & Uysal, 2017).

2.1. Meat samples

Minced meat packaged in high-oxygen modified air atmosphere was chosen as the model system because it is a highly perishable food, produced in relevant quantities and marketed conventionally in this package type. Although mixed minced pork and beef has a larger market share, pure pork was chosen for this study to keep the meat matrix as simple as possible by restricting it to one species. The standard storage temperature was set to 2 °C in accordance with European regulations (Regulation (EC) No 853/2004, 2004b). Two scenarios involving disruption to the cold chain were tested to simulate potential cooling failures during transportation or at the start of the retail stage.

Thirteen independent batches of minced pork were produced over a period of two years for this feasibility study. Each batch comprised the shoulders of ten animals as well as fat from a minimum of three animals. The pork shoulders and fat were acquired from a local slaughterhouse. Minced meat was produced within 24 h *postmortem*. To this end, the shoulders were deboned and cut into pieces. The pieces were pre-mixed with the added fat, which was also cut into pieces to ensure an even distribution of individual animals throughout the batch. Approximately 65-kg batches of minced pork were produced using 3 mm sieves in an automatic grinder (AW114 TYP 271, K + G Wetter, Biedenkopf, Germany). Immediately after production, 250-g portions of cylindrical-shaped minced pork were packed in polypropylene trays (227 × 178 × 40 mm) with a vacuum filler (VF50, Albert Handtmann Maschinenfabrik GmbH & Co. KG, Biberach, Germany) and sealed under a modified atmosphere of 70% O_2 and 30% CO_2 using a multi-layer film containing EVOH (PET/PP, 60 μm; VC999 Verpackungssysteme AG, Herisau, Switzerland) to ensure low gas permeability. Each batch provided samples for one shelf-life trial. In total, meat and fat from about 170 animals was used in this study.

2.2. Experimental design

Two series of three shelf-life trials each were used for calibration of the regression models by storing six batches at constant 2 °C for up to 17

days. In general, measurements were performed 8 times during the 17-d storage period (on days 1, 3, 6, 8, 10, 13, 15, 17), except for the first three calibration experiments for which additional measurements were performed on day 4 (9 days of sampling, Table 1).

The impact of cold chain disruptions (CCDs) on the 2 °C storage condition was investigated in seven independent experiments following the above-described scheme with 8 days of sampling. These provided the test and validation samples (Table 1). The first of the seven experiments was used to test whether 6-h and 12-h disruptions had an impact on minced meat, and its duration was restricted to 15 days (7 days of sampling). The following six trials were then used to directly compare samples exposed to a CCD of 6 h ($n = 3$) or 12 h (n = 3) with control samples stored at constant 2 °C. A CCD was simulated on day 2 of storage by moving all (1 trial) or a fraction (6 trials) of the minced meat packages from the 2 °C room for a period of 6 h or 12 h to a room that was climatized to 14 °C. That is, control and treated samples derived from the same production batch of minced meat for a CCD trial, but the samples of the CCD trials were independent of those used for the calibration trials. Therefore, the control samples of the CCD trials were used to validate the regression models.

The temperature in the cold storage room was recorded every 5 min throughout the storage period using Tinytag temperature loggers (model TGP-4505; Gemini Data Loggers, Chichester, UK). In addition, the temperatures of the cold storage room and of the minced pork (core and surface) were independently logged during the CCD periods using Almemo data loggers with two sensor types (models 2690–8 and 2890–9; Ahlborn Mess- und Regelungstechnik GmbH, Holzkirchen, Germany). The temperature in the cold storage room and in the core of the minced meat was measured with resistance-based temperature sensors (Pt 100–1), while the surface temperature was measured with a NiCr-Ni thermocouple. Temperature measurements were performed on two samples ($n = 2$) during each CCD period.

2.3. Microbial analysis

For total colony counts (TVC), one sample was analyzed per sampling day except for day 0, when samples were taken from five different areas of the freshly prepared batch of minced pork (approx. 65 kg) to assess the variation of microbial cell counts in the food product. Minced pork samples were mashed to obtain reproducible cross-sections of the meat product. Total colony counts of aerobically growing mesophilic microorganisms were determined according to DIN EN ISO 4833-2:2022-05 standards (DIN - German Institute for Standardization, 2022). In brief, 20 g of minced pork were transferred to a sterile plastic bag with a filter (stomacher bag) and mixed with 180 ml of peptone salt solution (NaCl 8.5 g/l, casein 1.0 g/l), followed by homogenization for two minutes using a stomacher. Homogenates were serially diluted tenfold with peptone salt solution. Samples (1 ml or 0.1 ml each) were plated on the surface of solidified plate count agar (1.5% *w/v*) either manually using a glass spreader or automatically using a spiral plater (Don Whitley Scientific Limited, Bingley, UK). After incubation at 30 °C for 72 ± 2 h, all visible colonies grown on the plate surface were automatically counted using an aCOLyte3 HD cell counter (Synbiosis, Cambridge, UK). Microbial counts were expressed as the number of colony forming units (cfu) per g of sample.

Table 1
Overview of storage experiments at 2 °C for calibration (Cal), test (Test) and validation (Val) with duration of cold chain disruptions (CCD) at 14 °C on day 2 of storage in hours. Number of measurement days per trial (Days of sampling) and number of samples (Samples) for total viable plate counts (TVC) and fluorescence (FL) measurements through package and with opened samples with sums (Σ). Triplicate samples were used for fluorescence measurements, except for the first trial* when only one sample was measured through the package. Numbers in brackets refer to lost samples and outliers.

Purpose	Trials	CCD (h)	Days of sampling	Samples		
				TVC	FL $_{\text{through package}}$	FL $_{\text{unpacked}}$
Cal	3	0	9	27	63*	80(1)
	3	0	8	24	72	72
	Σ 6			Σ 51	Σ 135	Σ 152
Test/ Val	1	0/6/ 12	1/6/6	13	3/18/18	3/18/18
	3	0/6/−	8/7/−	45	72/63/−	72/63/−
	3	0/ −/12	8/−/7	45	72/−/62 (1)	72/−/60 (3)
	Σ 7			Σ 103	Σ 147/81/ 80	Σ 147/ 81/78

2.4. Fluorescence analysis

Fluorescence spectra were recorded with a portable fluorescence device (BFD-100, FreshDetect GmbH, Germany) with an excitation wavelength of 405 nm and a detection range of 460 to 900 nm. Three samples were measured on each measurement day per treatment through the package and after removing the foil (unpacked), except for the first experiment for which only one sample per day has been measured unpacked, otherwise always 3 samples per day and treatment through package and unpacked (condition). Spectra were collected at 11 randomly selected positions per sample and condition using auto exposure, which is adapting the integration time to the signal level. The fluorescence spectra were checked for outliers in a two-step process. Initially, the raw spectra were visually inspected for obvious outliers (no signal, saturation etc.) and then the typically 11 spectra were averaged to one mean spectrum per sample using Microsoft Excel 365 (Microsoft Corporation, Redmond, WA, USA). This resulted in 3 mean spectra per measurement day × treatment × condition. In doing so, the spectra of 3 samples had to be discarded as they showed no signal (Calibration: 1 spectrum on day 13, unpacked; Tests: 2 spectra on day 3, unpacked with 12-h CCD, see Table 1). The second step of outlier detection was performed with the averaged spectra (see next section).

2.5. Data processing

Partial least-squares regression (PLSR) was used to calculate calibration models for storage time and TVC. The full range mean fluorescence spectra served as X matrix and storage time or TVC as y vectors. For both variables, two models were calculated each using Solo Toolbox 9.1 (Eigenvector Research Inc., Manson, WA, USA): with data measured (i) through the package and (ii) after unpacking. Fluorescence spectra measured through the package were pre-processed with Savitzky-Golay smoothing (order 0, filter width 15), 1st derivative (order: 1, filter width 15), and mean centering and unpacked samples with Savitzky-Golay smoothing (order 0, filter width 7), baseline correction (automatic weighted least squares, order 2), standard normal variate normalization and mean centering. Both models for packaged samples had 5 latent variables and both models for unpacked samples had 7 latent variables. Multivariate outliers were identified using Hotelling T^2 scores and Q residuals calculated with the developed PLSR models (Joe Qin, 2003). No further outliers were found in the calibration data set, but one more sample of a 12-h CCD trial had to be discarded (through package and unpacked). Variable importance in projection (VIP) scores was tested to reduce the number of spectral channels. While this resulted in slightly better predictions for the storage time for opened samples, it led to a deterioration of the predictions of storage time for packed samples (RMESCV, RMSEP and R^2_{Pred}). VIP reduction had almost no effect on TVC predictions independent of the package condition. To ease comparison, models were calculated without VIP reduction as this did not generally improve model performance. Model calculations with support vector machine (SVM) yielded also no improvement of the model performance for any of the investigated scenarios.

In total, 135 samples were used to calibrate the PLSR model for fluorescence spectra measured through the package and 152 samples for

the PLSR model for opened packages. The control samples of the last seven experiments were used to validate the models trained with samples stored at 2 °C while the CCD-treated samples were used to evaluate how the actual state of the meat product was predicted by this model. The test data set comprised 147 control samples, 81 samples with 6-h CCD and 80 (78 unpacked) samples with 12-h CCD (see Table 1).

3. Results and discussion

3.1. Temperature monitoring

The logged temperature of the cold storage room was on average 1.84 ± 0.23 °C during the calibration experiments and 1.89 ± 0.25 °C during the validation experiments (controls). The elevated temperatures of the cold storage room during the CCD treatments were on average 13.4 ± 1.3 °C for the 6-h CCDs and 13.7 ± 0.8 °C for the 12-h CCDs (Supplementary Table A1). It is interesting to note that the elevated temperature during a CCD simulation was reached in the core of the minced pork with a delay of approximately 4.5 h (Supplementary Fig. A1). When returning the samples to the 2 °C environment, the minced pork cooled to approximately 4 °C within the first two hours. However, in total about 14 h were required to reach a constant 2 °C level.

3.2. Determination of storage time from fluorescence spectra

Regression of the fluorescence spectra against storage time yielded cross-validated calibration models with R^2_{cv} = 0.90 and 0.95 for measurements through the package and after unpacking, respectively. The correlation was higher after unpacking and the model error was accordingly better 1.18 d vs. 1.60 d through package, see Figs. 1A, 2A and Table 2. Therefore, results of validation and CCD tests are discussed separately for measurements through the package and after unpacking. The main difference between both measuring procedures is that scattering and reflection of the package foil increased the spectral background (see Appendix Figs. A4 to A9). Spectra measured through the package started generally at a background intensity level of 100 a.u., whereas unpacked samples started at 20 a.u. The higher intensity level increased the shot noise level.

3.3. Prediction of storage time through the package

The validation of the model with control samples from the seven CCD trials resulted in an R^2_{Pred} of 0.71 and an error of 3.1 d (RMSEP), Table 3. Predictions of the storage time were reasonable until day 13. After that time, the predictions became less accurate and showed high variation (Fig. 1B). In general, the samples had spoiled and were sensory inacceptable at that time of storage. Therefore, only the linear range was considered up to day 13. This resulted in an R^2_{Pred} of 0.83 and improved the RMSEP to 1.7 d, see Table 3.

Results of the tests with 6 and 12-h CCDs showed that samples which underwent a CCD were rated slightly older than those which had been stored constantly at 2 °C (Fig. 1C and D, respectively). For the 6-h CCD, the effect was observable until storage day 10. Then, the predictions were in line with the calibration. For the 12-h CCD, the offset was observed until day 13 and showed afterwards a similar scatter as in the validation (Fig. 1B). The effect, i.e. the bias increased with the duration of the CCD, see Table 3. The bias is indicating the uprating of the storage time by fluorescence analysis of those samples, which underwent a CCD. Considering the range until spoilage, the predicted age of samples with 6 or 12 h of CCD was about 1 or 2.5 d older than the actual storage time. Both effects were not significant given the model error of 1.6 d. It is

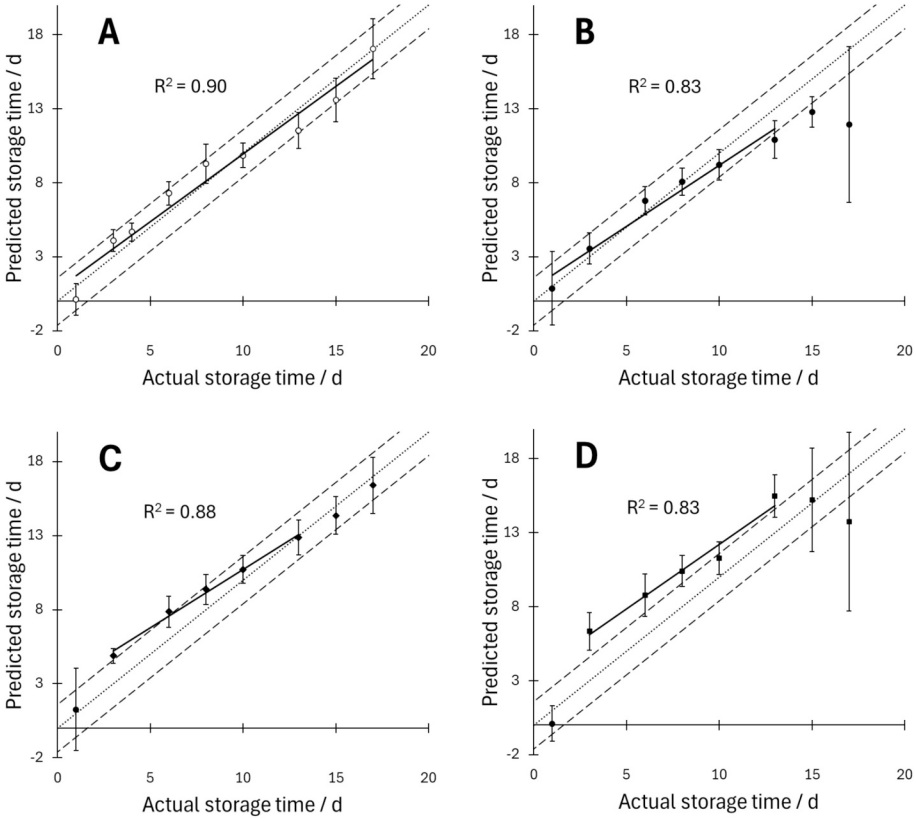

Fig. 1. Averaged predicted storage time vs. actual storage time for samples measured through the package. A: Calibration data (open symbols), B: validation with control samples stored at 2 °C, C: test with 6 h CCD, D: test with 12 h CCD (test data with filled symbols). Error bars indicate one standard deviation, solid line: linear regression, dotted line: identity, dashed lines: +/− RMSECV of the calibration model.

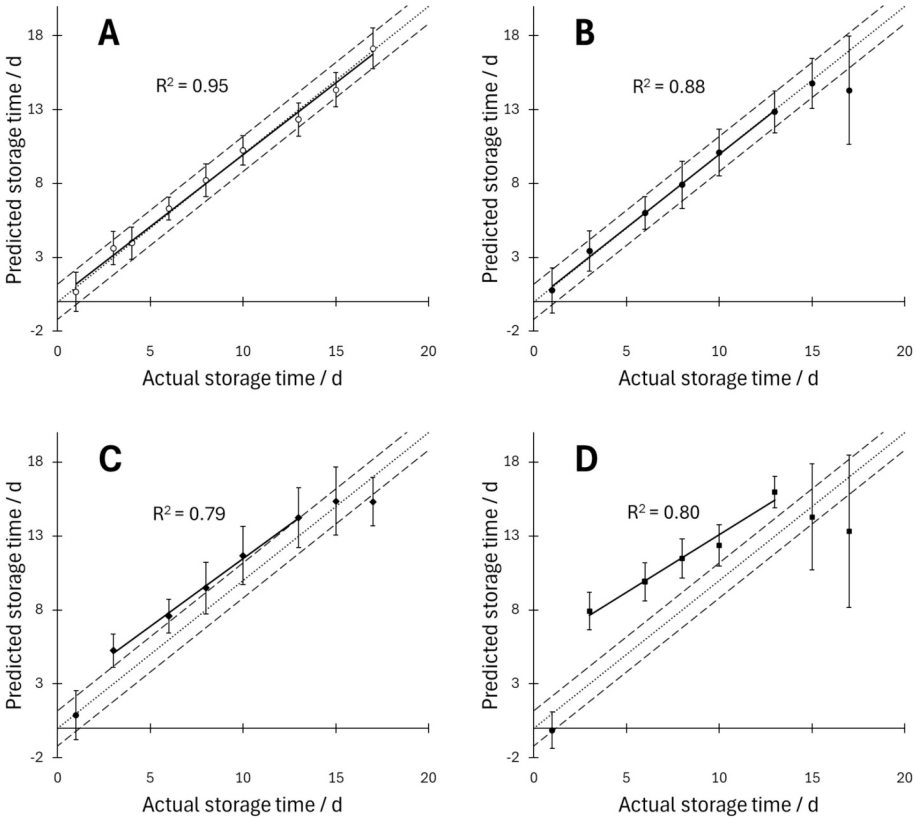

Fig. 2. Averaged predicted storage time vs. actual storage time for unpacked samples. Calibration (open symbols), test data (filled symbols). A: calibration, B: validation at 2 °C, C: test with 6 h CCD, D: test with 12 h CCD. Error bars indicate one standard deviation, solid line: linear regression, dotted line: identity, dashed lines: +/− RMSECV of the calibration model.

Table 2
Figures of merit of PLSR models of fluorescence spectra vs. storage time for measurements through the package and unpacked. Number of latent variables (LV), coefficient of determination R^2_{CV} of cross-validation (CV), and root mean squared error of calibration (RMSEC) and cross validation (RMSECV).

PLSR calibration	LVs	R^2_{CV}	RMSEC (d)	RMSECV (d)
Trough package	5	0.90	1.44	1.60
Without package	7	0.95	0.98	1.18

Table 3
Results of the PLSR predictions of storage time from fluorescence spectra for measurements through the package for the storage time 1–13 d and 1–17 d. Coefficient of determination R^2_{Pred}, root mean squared error (RMSEP) and bias of prediction.

Storage range	1–13 d			1–17 d		
Test data	R^2_{Pred}	RMSEP (d)	Bias (d)	R^2_{Pred}	RMSEP (d)	Bias (d)
Control 2°C	0.83	1.68	−0.27	0.71	3.06	−1.11
6 h CCD	0.88	1.65	1.14	0.90	1.64	0.68
12 h CCD	0.83	2.83	2.46	0.53	3.52	1.51

noteworthy that the largest effect was observed the day after the CCD occurred.

3.4. Prediction of storage time after unpacking

Compared to measurements taken through the package, the calibration and control samples stored at a constant temperature of 2 °C were much better predicted after the samples had been unpacked (Fig. 2A and B). Considering again only the first 13 days of storage, the R^2_{Pred} improved to 0.88, the RMSEP decreased to 1.4 d and the prediction bias was close to zero (Table 4). The differences between control and CCD groups were more pronounced when samples were measured unpacked and the negative effect of spoiled samples on the ability to predict the storage day beyond day 13 was confirmed (Fig. 2B, C and D). The bias was 1.7 d and 3.5 d for the 6 h and the 12-h CCD, respectively (Table 4). In view of the model error of 1.18 d, the effect of a 6-h CCD was insignificant, but the bias of a 12-h CCD was significantly different from the control samples.

3.5. Bacterial growth kinetics

Bacterial growth kinetics measured via TVC revealed high variability between batches. While the mean growth kinetics of the calibration samples showed a long lag phase and moderate min-max spread of about 2 log units during exponential growth (Fig. 3A), the test groups showed on average smaller (Fig. 3C) or higher growth rates (Fig. 3B and D). The differences between measured minimum and maximum TVC were less than 1 log unit for the experiments with 6-h CCD and up to 3.5 log units for the experiments with 12-h CCD. During the first 10 days, the mean

Table 4
Results of the PLSR predictions of storage time from fluorescence spectra for measurements of unpacked samples for the storage time 1–13 d and 1–17 d. Coefficient of determination R^2_{Pred}, root mean squared error (RMSEP) and bias of prediction.

Storage range	1–13 d			1–17 d		
Test data	R^2_{Pred}	RMSEP (d)	Bias (d)	R^2_{Pred}	RMSEP (d)	Bias (d)
Control 2°C	0.88	1.42	0.01	0.85	2.09	−0.36
6 h CCD	0.79	2.31	1.65	0.80	2.29	1.09
12 h CCD	0.80	3.79	3.48	0.39	4.08	2.07

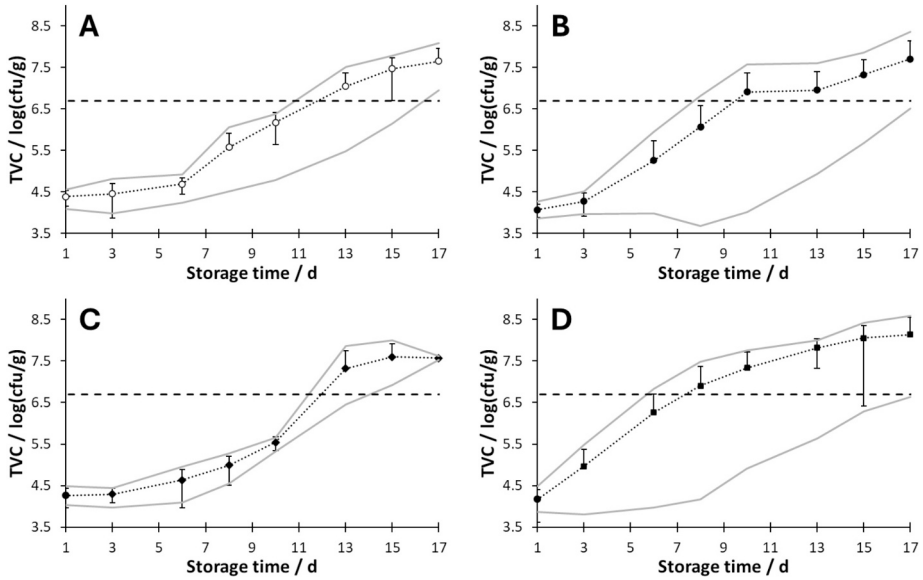

Fig. 3. Averaged measured total viable count (TVC) in log (cfu/g) for A: calibration, B: validation with control samples, C: test samples with 6 h CCD and D: test samples with 12 h CCD. Error bars represent one standard deviation (lower bars were omitted when the numbers exceeded the mean value), dotted lines indicate the average bacterial growth kinetics, grey lines: measured min/max TVC per measurement day. Dashed line: threshold of 5×10^6 cfu/g.

TVC of the 6-h CCD group (C) increased slower compared with the calibration samples (A). In contrast to this, samples with a CCD of 12 h (D) grew exponentially on average already on day 3. The large TVC spread observed in Fig. 2B is due to the delayed growth of the 6-h CCD reference samples and the faster growth of the 12-h CCD reference samples. The observed batch variability limited the accuracy of TVC predictions (see 3.7 and Fig. 5).

It is remarkable that the linear trend in the predicted storage time (Figs. 1 and 2) was not much influenced by the observed variations of TVC (Fig. 3). On day 13 of storage, the TVC of the samples always exceeded the threshold of 5×10^6 cfu/g. For some test experiments with 12-h CCD, the threshold was already reached at day 8 of storage (with CCD) or day 10 (control) (Fig. 3B and D). This value is regarded as the upper microbiological limit (M) for TVC at the end of the minced meat production process (Commission Regulation (EC) No 2073/2005 on microbiological criteria for foodstuffs, 2005).

3.6. Comparison of predicted storage time and measured TVC

In Figs. 1–3, mean results of the measurements were compared per group (calibration, control and CCDs). However, we have to cope with high batch-to-batch variations of the TVC kinetics. To compensate for

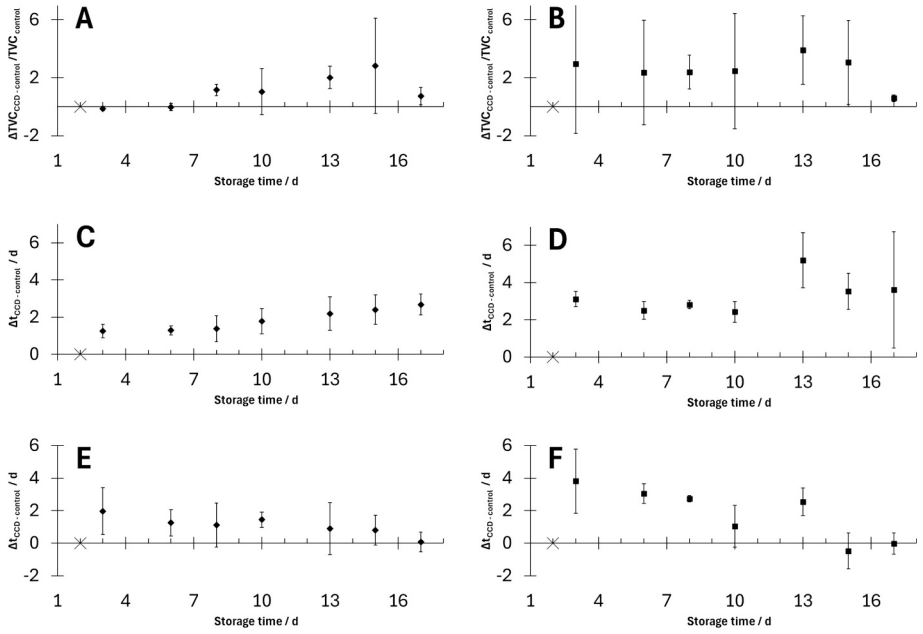

Fig. 4. Comparison of the average differences in total viable count (ΔTVC) and predicted storage time (Δt) between the CCD-treated samples and their respective reference samples from the same batches (left: 6 h CCD; right: 12 h CCD). Differences in TVC are calculated relative to the TVC of the controls (A, B) while the average difference in predicted storage time is stated in days between samples that experienced CCD and their respective control samples (i.e. from the same batch and day), measured through the package (C: 6 h CCD; D: 12 h CCD). The same as before but measured without package (E: 6 h CCD and F: 12 h CCD). ✕ indicates the point in time of the CCD and the error bars denote one standard deviation.

differences in factors such as the animal, its origin and TVC, the differences between the CCD test measurements and the respective controls were calculated individually for each batch, for both, TVC and predicted storage time, and then averaged. Thus, only changes related to the duration of the CCD are displayed (Fig. 4: 6 h on the left and 12 h on the right). For TVC, the difference was calculated relative to the TVC of the control (Fig. 4A and B for CCD of 6 h and 12 h, respectively). The 6-h CCDs had no influence on the TVC for the first 6 days of storage and TVC showed on tendency an increase beyond day 7. Whereas the 12-h CCD led to an almost constant relative increase of TVC from day 3 onwards, that is, directly after the CCD. However, none of these effects was significant given the observed large variances of TVC data.

Correspondingly, differences of the predicted storage times between the reference and treated samples were calculated for each batch of 6-h and the 12-h CCDs using fluorescence spectra measured through the package (Fig. 4C and D, respectively). For the 6-h CCD, the overestimation of the storage time was +1.3 d for the first 8 days, increasing afterwards to +2.7 d. For the 12-h CCD, the overestimation was between +2.4 and + 3 d until day 10, with high variation at the end of the storage period. The overvaluation of storage time was insignificant for the 6-h CCD, except for day 10, whereas the effect was significant for the 12-h CCD on the days 3, 8 and 13.

Samples, which were measured without package showed a different trend (Fig. 4E and F). While the predicted storage time was on average initially overestimated by 1.5 d and 4 d for the 6 h and the 12-h CCD, respectively, this difference decreased over time as the samples spoiled. The effect was insignificant for the 6-h CCD and significant for the 12-h CCD at the first days after the CCD (3, 6, 8). The exact reasons for the different behavior of samples measured through the package and after opening the package are not clear. Spectra measured through the package showed a higher broadband background and higher signal intensities compared to spectra, which were measured without package (see appendix, Figs. A4–A9). It is possible that this background, especially the observed etaloning, is interfering with the detected signals. Another explanation is that opening the package is standardizing the atmosphere to 21% oxygen, while the fluorescence measurements in the package are modulated by variations in the oxygen concentration. Fluorescence intensities of Zn-PPIX were shown to be effectively quenched by oxygen depending on the package type (Durek et al., 2012). The authors reported intensities (in a.u.) of 500 for vacuum (absence of O_2), 300 for aerobic package (ca. 20% O_2) and 40 for MAP (70% O_2 / 30% CO_2) (Durek et al., 2012). Note that in Figs. A4–A9 absolute signal intensities cannot be compared due to autoexposure. Tofteskov et al. observed a decrease in the oxygen concentration in the sample's headspace over time towards the end of the storage period due to microbial activity or oxidation (Tofteskov, Tørngren, Bailey, & Hansen, 2019). Accordingly, we attribute the strong increase of fluorescence towards the end of the storage period, particularly, at days 15 and 17 to a cessation of quenching by oxygen. i.e. oxygen depletion (see Figs. A4–A9 red and black spectra). This could also account for larger variations observed towards the end of the storage period.

Given the correlation between fluorescence spectra and TVC (Durek et al., 2012; Grimmler et al., 2018; Schneider et al., 2008), it was important to establish whether the prediction of storage time was related to TVC or vice versa. The fact that overvaluation of storage time in the 6-h CCD was detected from day 3 onwards (Fig. 4C and E), while bacterial counts did not increase faster than the control until day 8 (Fig. 4A) suggests that porphyrins in the meat matrix are responsible for the fluorescence detection rather than bacteria. Conversely, the overestimation of the predicted storage time increased from day 8 onwards, which was accompanied by an increase in TVC (Fig. 4A and C). This indicates that the predicted storage time and the TVC could be related. During the 12-h CCD experiment the storage time was overestimated from day 3 onwards, and the TVC also increased from day 3 onwards (Fig. 4B and D). In this case, the influence of TVC cannot be excluded.

In general, TVC was correlated with storage time between $r^2 = 0.48$ and 0.89 (Table 5). The r^2s were always higher for the longer storage period due to the larger spread. A breakdown of the correlation was observed for the control samples stored at 2 °C and for the 12-h CCD, which was in accordance with the higher variations of the bacterial growth kinetics of these samples (Fig. 3B and D). In contrast to this, the correlation of actual and predicted storage time yielded r^2s between 0.79 and 0.92 for the period up to 13 d disregarding of the type of measurement (through package or unpacked).

3.7. Determination of TVC from fluorescence spectra

PLSR regression of the fluorescence spectra against TVC with the calibration data set yielded cross-validated calibration models with $R^2_{cv} = 0.76$ and 0.83 for measurements through the package and after unpacking, respectively (Table 6 and Fig. 5A). The performance was in keeping with previous findings for unpacked samples (Grimmler et al., 2018). As with the storage time, the measurements of unpacked samples yielded always better predictions than measurements through the package (RMSECVs 0.54 and 0.63 log(cfu/g) for unpacked and packaged samples, respectively). Therefore, we restrict the discussion here to unpacked samples (for measurements through the package see appendix).

3.8. Prediction of TVC from fluorescence spectra

In contrast to the storage time, the validation of the TVC model with the control samples stored at 2 °C from the six trials of the test data set failed: the R^2_{Pred} dropped to 0.69 (Fig. 5B). The samples of the 6-h CCD were better predicted ($R^2_{Pred} = 0.80$), whereas the model turned out to be unable to predict samples correctly which underwent a CCD of 12 h ($R^2_{Pred} = 0.48$). The predictions were only good as long the underlying bacterial growth kinetics were similar to the average kinetic in samples used for the calibration (Fig. 5C). As the variation of TVC increased, predictions became inaccurate (Fig. 5B, D and Table 7). That samples of the 6-h CCD trials were correctly predicted is due to the fact, that the underlying bacterial growth kinetics were closer to those determined in the samples that were used for the model calibration. Correlations were lower when samples were measured through the package: $R^2_{Pred} = 0.76$, 0.35, 0.71 and 0.18 (from A to D, see Appendix Fig. A2 and Table A2). These low coefficients of determination do not support the thesis that fluorescence spectra predict TVC directly rather than that TVC is indirectly predicted via the storage time. This is further supported by a comparison of the regression vectors for TVC and storage time, which both evaluate essentially the same spectral features. Therefore, TVC predictions from fluorescence spectra are too inaccurate for application in practice considering typical batch variabilities.

In contrast to TVC, correlations between the predicted and the actual storage times were high (0.71–0.88) supporting a tight correlation. We

Table 5
Coefficients of determination r^2 of cross-correlations of measured total viable count (TVC) and actual storage time as well as actual and predicted storage time for the two storage ranges.

Measured TVC	Calibration	Control 2°C	6 h CCD	12 h CCD
	Actual storage time			
1–17 d	0.83	0.68	0.89	0.55
1–13 d	0.70	0.48	0.80	0.48
Actual storage time	Predicted storage time (trough package)			
1–17 d	0.90	0.71	0.90	0.53
1–13 d	0.87	0.83	0.88	0.83
	Predicted storage time (unpacked)			
1–17 d	0.95	0.85	0.80	0.39
1–13 d	0.92	0.88	0.79	0.80

Table 6
Figures of merit of PLSR correlation of fluorescence spectra vs. TVC for measurements through the package and unpacked. Number of latent variables (LVs), coefficient of determination R^2_{CV} of cross-validation, root mean squared error of calibration (RMSEC) and cross validation (RMSECV).

PLSR calibration	LVs	R^2_{CV}	RMSEC (log(cfu/g))	RMSECV (log(cfu/g))
Trough package	5	0.76	0.57	0.63
Without package	7	0.83	0.47	0.54

assume that the storage time is indirectly predicted from fluorescence spectra by time-temperature dependent changes within the meat matrix causing an increase of the Zn-PPIX fluorescence during storage. To illustrate this effect, difference spectra were calculated for calibration, validation, 6-h CCD and 12-h CCD between the unprocessed mean fluorescence spectra of unpacked samples per storage day and the corresponding spectra of day 1. Calibration and validation spectra (Fig. 6A and B) with storage at constant 2 °C showed a moderate increase of the Zn-PPIX fluorescence at 589 nm and a decrease of the PPIX fluorescence at 637 nm (with reference to day 1 of storage). In contrast to this, CCDs of 6 and 12 h (Fig. 6C and D, respectively), resulted in a stronger increase in the Zn-PPIX fluorescence and the development of a second signal at 650 nm which could be attributed to the second signal of Zn-PPIX at 645 nm. The signal is compensated by the decreasing signal of PPIX at 637 nm during the first 6 days and appears therefore long-wave shifted. The signal at 650 nm also points at a formation of Mg-PPIX which has fluorescence signals at 595 and 650 nm (Jaschke, Hardjasa, Digby, Hunter, & Beatty, 2011; Schneider et al., 2008). This is further underpinned by a peak shift of the 589 nm signal to 592 nm with storage time. Fluorescence spectra measured through the package showed essentially the same trend (Fig. A3A–D).

4. Summary

The results demonstrated the potential of fluorescence spectroscopy to reveal a CCD of MAP-packed minced pork. However, predictions were generally more accurate if the spectra were measured on unpacked samples than if measured through the package, possibly due to the higher spectral background of packed samples. The calibration models were used to evaluate the storage time of samples that were stored at a constant temperature of 2 °C. Samples whose cold chain was disrupted for 6 or 12 h on day 2 of storage (at 14 °C) were systematically predicted to be older than they actually were. The duration of the disruption played a role: 6 h of CCD at 14 °C resulted in an additional 1–2 d, while 12 h at 14 °C resulted in an additional 3–4 d compared to the constant storage at 2 °C. This effect was observed from the day after the disruption until the samples had spoiled (day 13). In this study, the disruption for 6 h was detectable by tendency via storage time, while TVC did not increase significantly. Samples with a 12-h disruption were predicted significantly older. Additionally, TVC increased on average faster after 12 h of CCD.

Table 7
Results of the PLSR predictions of TVC from fluorescence spectra for measurements through the package for the storage time 1–13 d and 1–17 d. Coefficient of determination R^2_{Pred}, root mean squared error of prediction (RMSEP).

Storage time	1–13 d		1–17 d	
Test data (unpacked)	R^2_{Pred}	RMSEP (log(cfu/g))	R^2_{Pred}	RMSEP (log(cfu/g))
Control 2°C	0.57	0.83	0.69	0.85
6 h CCD	0.76	0.89	0.80	0.80
12 h CCD	0.54	1.13	0.48	1.13

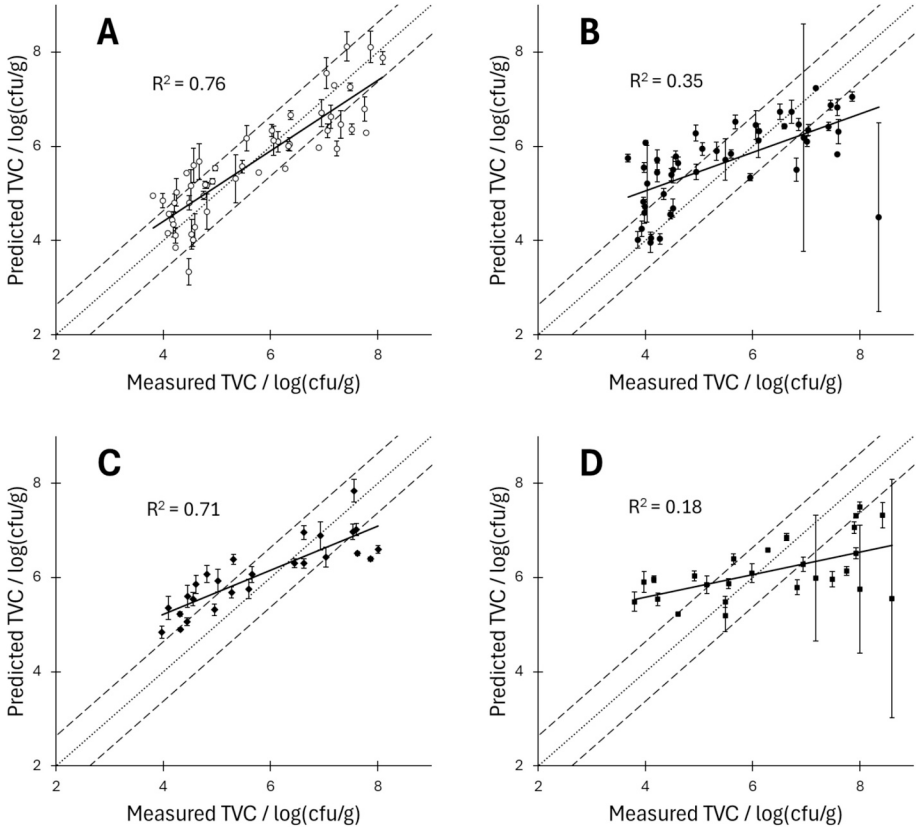

Fig. 5. Predicted TVC vs. measured TVC for unpacked samples. Calibration (open symbols), test data (filled symbols). A: calibration, B: validation at 2 °C, C: test with 6 h CCD, D: test with 12 h CCD. Average of triplicates per day and trial, error bars indicate one standard deviation, solid line: linear regression, dotted line: identity, dashed lines: +/− one RMSECV of the calibration model.

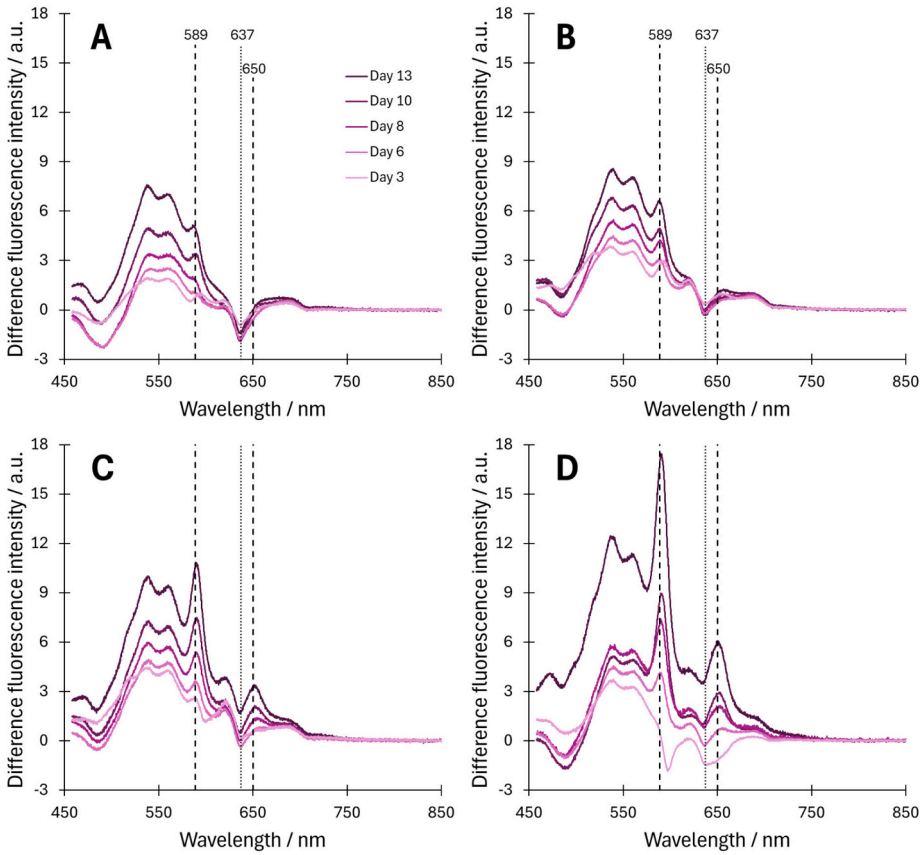

Fig. 6. Difference spectra of unpacked samples for calibration (A), validation (B), 6-h CCD (C) and 12-h CCD (D) calculated for each treatment between the unprocessed mean fluorescence spectra per storage day and the corresponding mean spectra of day 1. Vertical lines indicate fluorescence peak positions of Zn-PPIX (dashed) and PPIX (dotted).

5. Conclusions

This study suggest that fluorescence spectra do not measure the "age of the sample", rather that they evaluate the storage time at a constant reference temperature (here 2 °C) after preparation of the meat product. Notably, the fluorescence of Zn (and Mg) complexes of PPIX increased during storage. We hypothesize that the processes leading to the formation of these metal complexes or to the increase of their fluorescence were faster at higher temperatures such as during a CCD. This resulted in an overestimation of the storage time compared to storage at 2 °C. Given the low microbial burden immediately after minced meat production, the data indicate that primarily porphyrins of the meat matrix are measured via fluorescence spectroscopy. However, TVC at a higher level may influence the prediction of storage time. TVC kinetics revealed high variability between batches. In general, the correlations between fluorescence spectra and storage time were stronger than those between fluorescence spectra and TVC. This also suggests that TVC were not directly predicted from fluorescence spectra, but indirectly via the storage time and based on an average bacterial growth kinetic. If samples deviated from this average bacterial growth kinetic, TVC predictions became inaccurate. We conclude that the batch-to-batch variability in TVC impedes the generalization of TVC predictions from fluorescence spectra that were excited at 405 nm because deviations from the average bacterial growth kinetics can be eminent. This leads to inacceptable errors.

However, this study demonstrated the potential of fluorescence spectroscopy for detection of cold chain disruptions in a fresh meat product for samples produced on a pilot scale after unpacking. As the duration of the disruption had a measurable effect, this could be useful to evaluate the impact of a cold chain disruption on the shelf life of a product in real time, or to examine time-temperature effects during production or storage. For industrial and retail application, non-invasive measurements through packages are required and shorter temperature abuses should be also considered. Adoption for industrial application is currently limited by the prediction accuracy of models which must be improved, especially for measurements through package. This should include modifications to the device, for example to reduce the spectral background and to increase the fluorescence signal using blue laser diodes for excitation. The calibration should be supplemented with spectra measured through other package materials, and model calculations can be further refined when using larger databases and including temperature as a covariate. Additional studies are required to demonstrate the application of this approach to samples produced on an industrial scale.

Consent form

This study does not involve human or animal experimentation.

CRediT authorship contribution statement

Johannes Schlosser: Writing – original draft, Visualization, Methodology, Investigation, Formal analysis, Data curation. **Martin Mühling:** Writing – review & editing, Investigation, Conceptualization. **Sonja Lick:** Supervision, Resources, Data curation. **Heinar Schmidt:** Writing – review & editing, Supervision, Resources, Conceptualization.

Declaration of competing interest

The authors declare that they have no known competing financial interests or personal relationships that could have appeared to influence

the work reported in this paper.

Acknowledgements

The project was supported by funds of the Federal Ministry of Food and Agriculture (BMEL) based on a decision of the Parliament of the Federal Republic of Germany. The Federal Office for Agriculture and Food (BLE) provided coordinating support for artificial intelligence (AI) in agriculture as funding organization, grant numbers 28DK126C20 and 28DK126E20. We thank Manfred Behrschmidt, Josef Haida and Marco Zäh for preparing the meat samples, Larissa Stumpf-Krellowetz, Shevellarasi Ganesha-Rajan, Susanne Büchs and Milena Anders for the microbiological analyses, Daniel Schmidt for the temperature measurements during cold chain disruptions and Kathrin Fiedler for assistance with spectra acquisition and data curation.

Appendix A. Supplementary data

Supplementary data to this article can be found online at https://doi.org/10.1016/j.meatsci.2026.110048.

Data availability

Data will be made available on request.

References

Albrecht, A., Ibald, R., Raab, V., Reichstein, W., Haarer, D., & Kreyenschmidt, J. (2020). Implementation of time temperature indicators to improve temperature monitoring and support dynamic shelf life in meat supply chains. *Journal of Packaging Technology and Research, 4*(1), 23–32. https://doi.org/10.1007/s41783-019-00080-x

Bartáková, K., Bursova, S., Necidová, L., Haruštiaková, D., Zouharová, A., Vorlová, L., & Klimešová, M. (2022). The effect of cold chain disruption on the microbiological profile of chilled fish. *Journal of Microbiology, Biotechnology and Food Sciences*. , Article e9883. https://doi.org/10.55251/jmbfs.9883

Bruckner, S., Albrecht, A., Petersen, B., & Kreyenschmidt, J. (2012). Influence of cold chain interruptions on the shelf life of fresh pork and poultry. *International Journal of Food Science & Technology, 47*(8), 1639–1646. https://doi.org/10.1111/j.1365-2621.2012.03014.x

Candoğan, K., Altuntas, E. G., & İğci, N. (2021). Authentication and quality assessment of meat products by Fourier-transform infrared (FTIR) spectroscopy. *Food Engineering Reviews, 13*(1), 66–91. https://doi.org/10.1007/s12393-020-09251-y

Commission Regulation (EC). (2005). No 2073/2005 on microbiological criteria for foodstuffs. *Official Journal of the European Union*, 1–26. L 338, 22.12.2005.

Deng, Z., Sun, S., Shi, Y., Hu, Y., Lü, X., & Shan, Y. (2024). Effect of cold chain interruption on the metabolic composition and quality properties of fresh beef. *Food Science of Animal Products, 2*(2), Article 9240060. https://doi.org/10.26599/FSAP.2023.9240060

Derens-Bertheau, E., Osswald, V., Laguerre, O., & Alvarez, G. (2015). Cold chain of chilled food in France. *International Journal of Refrigeration, 52*, 161–167. https://doi.org/10.1016/j.ijrefrig.2014.06.012

DIN - German Institute for Standardization. (2022). *Microbiology of the food chain – Horizontal method for the enumeration of microorganisms – Part 2: Colony count at 30° C by the surface plating technique*. Berlin: DIN Media GmbH.

Durek, J., Bolling, J. S., Knorr, D., Schwägele, F., & Schlüter, O. (2012). Effects of different storage conditions on quality related porphyrin fluorescence signatures of pork slices. *Meat Science, 90*(1), 252–258. https://doi.org/10.1016/j.meatsci.2011.07.010

Durek, J., Fröhling, A., Bolling, J., Thomasius, R., Durek, P., & Schlüter, O. K. (2016). Non-destructive mobile monitoring of microbial contaminations on meat surfaces using porphyrin fluorescence intensities. *Meat Science, 115*, 1–8. https://doi.org/10.1016/j.meatsci.2015.12.022

EFSA Panel on Biological Hazards. (2016). Growth of spoilage bacteria during storage and transport of meat. *EFSA Journal, 14*(6), Article e04523. https://doi.org/10.2903/j.efsa.2016.4523

Fengou, L.-C., Mporas, I., Spyrelli, E., Lianou, A., & Nychas, G.-J. (2020). Estimation of the microbiological quality of meat using rapid and non-invasive spectroscopic sensors. *IEEE Access, 8*, 106614–106628. https://doi.org/10.1109/ACCESS.2020.3000690

Grimmler, C., Kuhfuß, T., Heiden, M., & Schmidt, H.[. H.]. (2018). Non-invasive assessment of the bioburden of minced pork using a hand-held fluorescence device. *TM. - Technisches Messen, 85*(3), 177–183. https://doi.org/10.1515/teme-2017-0092

Jaschke, P. R., Hardjasa, A., Digby, E. L., Hunter, C. N., & Beatty, J. T. (2011). A BchD (magnesium chelatase) mutant of *rhodobacter sphaeroides* synthesizes zinc bacteriochlorophyll through novel zinc-containing intermediates. *Journal of Biological Chemistry, 286*(23), 20313–20322. https://doi.org/10.1074/jbc.M110.212605

Jo, K., Lee, S., Jeong, S.-K.-C., Lee, D.-H., Jeon, H., & Jung, S. (2024). Hyperspectral imaging–based assessment of fresh meat quality: Progress and applications. *Microchemical Journal, 197*, Article 109785. https://doi.org/10.1016/j.microc.2023.109785

Joe Qin, S. (2003). Statistical process monitoring: Basics and beyond. *Journal of Chemometrics, 17*(8–9), 480–502. https://doi.org/10.1002/cem.800

Kumar, D., Singh, R. K., & Layek, A. (2020). Cold chain and its application. In K. Kumar, & J. P. Davim (Eds.), *Management and industrial engineering. Supply chain intelligence* (pp. 63–80). Cham: Springer International Publishing. https://doi.org/10.1007/978-3-030-46425-7_4.

Mercier, S., Villeneuve, S., Mondor, M., & Uysal, I. (2017). Time-temperature management along the food cold chain: A review of recent developments. *Comprehensive Reviews in Food Science and Food Safety, 16*(4), 647–667. https://doi.org/10.1111/1541-4337.12269

Necidová, L., Zouharová, A., Haruštiaková, D., Bursová, Š., Bartáková, K., & Golian, J. (2024). The effect of cold chain disruption on the microbiological profile of chilled chicken meat. *Poultry Science, 103*(12), Article 104290. https://doi.org/10.1016/j.psj.2024.104290

Oto, N., Oshita, S., Makino, Y., Kawagoe, Y., Sugiyama, J., & Yoshimura, M. (2013). Non-destructive evaluation of ATP content and plate count on pork meat surface by fluorescence spectroscopy. *Meat Science, 93*(3), 579–585. https://doi.org/10.1016/j.meatsci.2012.11.010

Pandian, A. T., Chaturvedi, S., & Chakraborty, S. (2021). Applications of enzymatic time–temperature indicator (TTI) devices in quality monitoring and shelf-life estimation of food products during storage. *Journal of Food Measurement and Characterization, 15*(2), 1523–1540. https://doi.org/10.1007/s11694-020-00730-8

Qu, C., Li, Y., Du, S., Geng, Y., Su, M., & Liu, H. (2022). Raman spectroscopy for rapid fingerprint analysis of meat quality and security: Principles, progress and prospects. *Food Research International (Ottawa, Ont.), 161*, Article 111805. https://doi.org/10.1016/j.foodres.2022.111805

Regulation (EC). (2004a). No 852/2004. *Official Journal (OJ)*, 1–54. Reference: OJ L 139, 30.4.2004.

Regulation (EC). (2004b). No 853/2004. *Official Journal (OJ)*, 55–205. Reference: OJ L 139, 30.4.2004.

Schneider, J., Wulf, J., Surowsky, B., Schmidt, H.[. H.]., Schwägele, F., & Schlüter, O. (2008). Fluorimetric detection of protoporphyrins as an indicator for quality monitoring of fresh intact pork meat. *Meat Science, 80*(4), 1320–1325. https://doi.org/10.1016/j.meatsci.2008.06.007

So, J.-H., Joe, S.-Y., Hwang, S.-H., Jun, S., & Lee, S.-H. (2021). Analysis of the temperature distribution in a refrigerated truck body depending on the box loading patterns. *Foods (Basel, Switzerland), 10*(11). https://doi.org/10.3390/foods10112560

Sohail, M., Sun, D.-W., & Zhu, Z. (2018). Recent developments in intelligent packaging for enhancing food quality and safety. *Critical Reviews in Food Science and Nutrition, 58*(15), 2650–2662. https://doi.org/10.1080/10408398.2018.1449731

Tofteskov, J., Tørngren, M. A., Bailey, N. P., & Hansen, J. S. (2019). Modelling headspace dynamics in modified atmosphere packaged meat. *Journal of Food Engineering, 248*, 46–52. https://doi.org/10.1016/j.jfoodeng.2018.12.013

Turgut, S. S., Myustedzhebov, A., & Feyissa, A. H. (2025). Low-cost multispectral sensor reveals cold chain breaks, meat type, and storage time in chicken meat samples. *Food Control, 167*, Article 110816. https://doi.org/10.1016/j.foodcont.2024.110816

Wang, W., Jiang, F., Zhang, L., Zhu, X.-L., & Wu, W.-Q. (2025). Screening and identification of deterioration markers in lean and fatty pork by metabolomics. *LWT, 215*, Article 117283. https://doi.org/10.1016/j.lwt.2024.117283

Yousefi, H., Su, H.-M., Imani, S. M., Alkhaldi, K., Filipe, C. D. M., & Didar, T. F. (2019). Intelligent food packaging: A review of smart sensing technologies for monitoring food quality. *ACS Sensors, 4*(4), 808–821. https://doi.org/10.1021/acssensors.9b00440